

$B_s \rightarrow \ell^+ \ell^-$ in a model II 2HDM and MSSM

Chao-Shang HUANG^{a*}, LIAO Wei^{a†}, Qi-Shu YAN^{b‡}, and Shou-Hua ZHU^{a,c§}

^aInstitute of Theoretical Physics, Academia Sinica, 100080 Beijing, China

^b Physics Department of Tsinghua University, 100080 Beijing, China

^c Institut für Theoretische Physik, Universität Karlsruhe, D-76128 Karlsruhe, Germany

Abstract

In this paper we analyze the process $B_s \rightarrow \ell^+ \ell^-$ in a model II 2HDM and MSSM. All the leading terms of Wilson coefficients relevant to the process are given in the large $\tan\beta$ limit. It is shown that the decay width for $B_s \rightarrow \ell^+ \ell^-$ depends on all parameters except m_{A^0} in the 2HDM. The branching ratio of $B_s \rightarrow \mu^+ \mu^-$ can reach its experimental bound in some large $\tan\beta$ regions of the parameter space in MSSM because the amplitude increases like $\tan^3\beta$ in the regions. For $\ell=\tau$, the branching ratio can even reach 10^{-4} in the regions. Therefore, the experimental measurements of leptonic decays of B_s could put a constraint on the contributions of neutral Higgs bosons and consequently the parameter space in MSSM.

PACS numbers: 13.20.He, 13.25.Hw

*E-mail : csh@itp.ac.cn

†E-mail: liaow@itp.ac.cn

‡E-mail : qsyang@mail.tsinghua.edu.cn

§ E-mail: huald@particle.uni-karlsruhe.de

1 Introduction

$B_s \rightarrow l^+l^-$, as one of flavor changing neutral current processes, is sensitive to structure of the standard model (SM) and new physics beyond SM, and is expected to shed light on the existence of new physics before the possible new particles are produced at colliders. Theoretically, the process is clean because only the nonperturbative quantity involved is of the decay constant of B_s and it is relatively easy to be calculated by so far well-known nonperturbative methods such as QCD sum rules, lattice gauge theory, Bethe-Salpeter approach, etc. Therefore, it provides a good window to probe new physics. Experimentally, the 95% confidence level upper bound on the $B_s \rightarrow \mu^+\mu^-$ branching fraction has been given [1]:

$$B_r(B_s \rightarrow \mu^+\mu^-) < 2.6 \times 10^{-6} \quad (1.1)$$

The planned experiments at B-factories are likely to measure branching fractions as low as 10^{-8} [2].

Compared to the rare decay $B \rightarrow X_s\gamma$, $B_s \rightarrow l^+l^-$ (as well as $B \rightarrow X_sl^+l^-$) is of more advantage for the study of the Higgs sector in the large $\tan\beta$ case in a model II two Higgs doublet model (2HDM) or supersymmetric models (SUSY) since the contributions to $B \rightarrow X_s\gamma$ coming from Higgs sector are indeed independent of $\tan\beta$ when $\tan\beta$ is larger than a few (say, 4).

The branching ratio for $B_s \rightarrow l^+l^-$ has been calculated in SM and beyond SM in a number of papers [3, 4, 8]. In a recent paper [9] the process in a model II 2HDM with large $\tan\beta$ is reanalyzed. It is correctly pointed out that the contributions of the box diagram to this decay at the leading order of $\tan\beta$ are missed and a minus for the contribution of A^0 penguin diagram involving H^\pm and W^\pm in the loop is also missed in the earlier literature [3, 4, 5]. However, there are some points in the paper which need to be clarified. First, the argument that the trilinear $H^\pm H^\mp H$ ($H=h^0, H^0$) couplings should not be considered as $\tan\beta$ enhanced is not correct, as we shall argue below. Second, although the contribution of box diagram is the same order as those of penguin diagrams in the large $\tan\beta$ limit it is numerically smaller than those of penguin diagrams and consequently the claim that the box diagram gives the dominant contribution in the 't Hooft-Feynman gauge is not true. In the paper we shall give a detailed argument (as we know, there is no such argument presented in the literature) to show why their claim on $H^\pm H^\mp H$ couplings is not correct (see section 3). These arguments are important to clarify where are the disagreements in the literature and make one have a correct conclusion on the decay in 2HDM.

There are more box diagrams in SUSY than that in 2HDM. The contributions of box diagrams in the analysis in supersymmetric models are missed in the previous papers [6, 7, 8]. The contributions are also omitted in the refs.[14, 16] since they neglect the mass of a lepton in calculating Wilson coefficients. However, for $l=\mu, \tau$ the contributions in the large $\tan\beta$ case are important and consequently should not be neglected. In the paper we calculate the contributions to Wilson coefficients C_9, C_{Q_i} from the box diagrams and carry out a complete analysis in a model II 2HDM and SUSY with large $\tan\beta$.

The paper is organized as follows. Section 2 is devoted to the effective Hamiltonian responsible for $b \rightarrow sl^+l^-$. We calculate the contributions to Wilson coefficients from the box diagrams and give all the leading terms of Wilson coefficients in a model II 2HDM and SUSY with large $\tan\beta$ in section 3. In section 4 we present the numerical results. In section 5 conclusions are drawn. Finally the contributions to Wilson coefficients C_9, C_{Q_i} from individual diagrams in a 2HDM and MSSM are given in the appendix.

2 Effective Hamiltonian for $b \rightarrow s\ell^+\ell^-$

The effective Hamiltonian describing the flavor changing processes $b \rightarrow s\ell^+\ell^-$ can be defined as

$$H_{eff} = -\frac{G_F}{\sqrt{2}}\lambda_t\left(\sum_{i=1}^{10}C_i(\mu)O_i(\mu) + \sum_{i=1}^{10}C_{Q_i}(\mu)Q_i(\mu)\right). \quad (2.2)$$

where $\lambda_t = V_{tb}V_{ts}^*$, O_i s ($i = 1, \dots, 10$) are the same as those given in the ref.[10, 12]¹, and Q_i s come from exchanging neutral Higgs bosons and have been given in refs. [5, 6].

The QCD corrections to coefficients C_i and C_{Q_i} can be incorporated in the standard way by using the renormalization group equations. Q_i ($i = 1, \dots, 10$) does not mix with O_8, O_9 so that the evolution of C_8 and C_9 remains unchanged and are given in ref.[10]

$$\begin{aligned} C_8(m_b) &= C_8(m_W) + \frac{4\pi}{\alpha_s(m_W)}\left[-\frac{4}{33}(1 - \eta^{-11/23}) + \frac{8}{87}(1 - \eta^{-29/23})\right]C_2(m_W), \\ &= C_8(m_W) + 1.937C_2(m_W) \end{aligned} \quad (2.3)$$

$$C_9(m_b) = C_9(m_W). \quad (2.4)$$

It is obvious that operators O_i ($i = 1, \dots, 10$) and Q_i ($i = 3, \dots, 10$) do not mix into Q_1 and Q_2 and also there is no mixing between Q_1 and Q_2 . Therefore, the evolution of C_{Q_1}, C_{Q_2} is controlled by the anomalous dimensions of Q_1, Q_2 respectively.

$$\begin{aligned} C_{Q_i}(m_b) &= \eta^{-\gamma_Q/\beta_0}C_{Q_i}(m_W), \quad i = 1, 2, \\ &= 1.24C_{Q_i}(m_W) \end{aligned} \quad (2.5)$$

where $\gamma_Q = -4$ [11] is the one loop anomalous dimension of $\bar{s}_L b_R$, $\eta = \frac{\alpha_s(m_b)}{\alpha_s(m_W)} \approx 1.72$, and $\beta_0 = 11 - (2/3)n_f = 23/3$.

For the decay $B_s \rightarrow l^+l^-$, the matrix element of \mathcal{H}_{eff} is to be taken between vacuum and $|B_s^0\rangle$ state. Because

$$\langle 0 | \bar{s} \sigma^{\mu\nu} P_R b | B_s^0 \rangle = 0 \quad (2.6)$$

and the O_8 term in eq.(2.2) gives zero on contraction with the lepton bilinear due to $p_B^\mu = p_+^\mu + p_-^\mu$, only the operators O_9 and Q_i

$$O_9 = \bar{s}_L \gamma^\mu b_L \bar{l} \gamma_\mu \gamma_5 l, \quad (2.7)$$

$$O_{Q_1} = \bar{s}_L b_R \bar{l} l, \quad (2.8)$$

$$O_{Q_2} = \bar{s}_L b_R \bar{l} \gamma_5 l \quad (2.9)$$

are involved and the important thing we need to do is to calculate the Wilson coefficients of the operators at $\mu = m_W$. $C_9(m_W)$ has been calculated in SM [13], in a 2HDM [10] and in SUSY models [14, 16] respectively. $C_9(m_W)$ in the 2HDM is the same as that in SM for the large $\tan\beta$ scenario.

¹We follow the convention in ref.[10] for the indices of operators as well as Wilson coefficients. In the convention of ref.[12] O_8 (O_9) is changed into O_9 (O_{10}).

The box diagram contributions to $C_9(m_W)$ (as well as $C_8(m_W)$) in SUSY which are proportional to $\tan^2\beta$ are missed in the previous calculations [16, 6, 7, 8]. C_{Q_i} s have also been calculated in 2HDM [5, 4, 9] and in SUSY [6, 7]. However, some leading terms in the large $\tan\beta$ limit are missed in the previous papers. We shall calculate C_9 and C_{Q_i} at $\mu = m_W$ in the next section in order to give a complete and correct result.

By using the equations of motion for quark fields, we have

$$\langle 0 | \bar{s} \gamma_5 b | B_s^0 \rangle = i f_{B_s} \frac{m_{B_s}^2}{m_b + m_s} \quad (2.10)$$

where f_{B_s} is the decay constant of B_s defined by

$$\langle 0 | \bar{s} \gamma^\mu \gamma_5 b | B_s^0 \rangle = -i f_{B_s} p^\mu \quad (2.11)$$

Thus the effective Hamiltonian (2.2) results in the following decay amplitude for $B_s \rightarrow l^+ l^-$

$$A = \frac{G_F \alpha_{EM}}{2\sqrt{2}\pi} m_{B_s} f_{B_s} \lambda_t [C_{Q_1} \bar{u}v + (C_{Q_2} + 2\hat{m}_l C_9) \bar{u} \gamma_5 v], \quad (2.12)$$

where $\hat{m}_l = m_l/m_{B_s}$ and $m_{B_s} \approx m_b + m_s$ have been used. Then it is straightforward to obtain the branching ratio for $B_s \rightarrow l^+ l^-$

$$\begin{aligned} Br(B_s \rightarrow \ell^+ \ell^-) &= \frac{G_F^2 \alpha_{EM}^2}{64\pi^3} m_{B_s}^3 \tau_{B_s} f_{B_s}^2 |\lambda_t|^2 \sqrt{1 - 4\hat{m}_\ell^2} \\ &\times \left[(1 - 4\hat{m}_\ell^2) |C_{Q_1}|^2 + |C_{Q_2} + 2\hat{m}_\ell C_9|^2 \right], \end{aligned} \quad (2.13)$$

where τ_{B_s} is the B_s lifetime.

3 Wilson coefficients

3.1 In 2HDM

Consider two complex hypercharge $Y = 1$, $SU(2)_w$ doublet scalar fields, ϕ_1 and ϕ_2 . The Higgs potential which spontaneously breaks $SU(2) \times U(1)$ down to $U(1)_{EM}$ and conserves CP symmetry can be written in the following form [17]:

$$\begin{aligned} V(\phi_1, \phi_2) &= \lambda_1 (\Phi_1^\dagger \Phi_1 - v_1^2)^2 + \lambda_2 (\Phi_2^\dagger \Phi_2 - v_2^2)^2 \\ &+ \lambda_3 [(\Phi_1^\dagger \Phi_1 - v_1^2) + (\Phi_2^\dagger \Phi_2 - v_2^2)]^2 \\ &+ \lambda_4 [(\Phi_1^\dagger \Phi_1)(\Phi_2^\dagger \Phi_2) - (\phi_1^\dagger \Phi_2)(\Phi_2^\dagger \Phi_1)] \\ &+ \lambda_5 [\text{Re}(\Phi_1^\dagger \Phi_2) - v_1 v_2]^2 \\ &+ \lambda_6 [\text{Im}(\Phi_1^\dagger \Phi_2)]^2 \end{aligned} \quad (3.14)$$

Hermiticity requires that all parameters are real. If $\lambda_i \geq 0$ the potential is semi-positive and the minimum of the potential is at

$$\langle \Phi_1 \rangle = \begin{pmatrix} 0 \\ v_1 \end{pmatrix}, \quad \langle \Phi_2 \rangle = \begin{pmatrix} 0 \\ v_2 \end{pmatrix}, \quad (3.15)$$

thus breaking $SU(2) \times U(1)$ down to $U(1)_{EM}$. From the potential the mass eigenstates are easily found as follows. The charged Higgs states are

$$\begin{aligned} G^\pm &= \phi_1^\pm \cos \beta + \phi_2^\pm \sin \beta \\ H^\pm &= -\phi_1^\pm \sin \beta + \phi_2^\pm \cos \beta, \end{aligned} \quad (3.16)$$

where the mixing angle β is defined by $\tan \beta = v_2/v_1$. The CP-odd states are

$$\begin{aligned} G^0 &= \sqrt{2}[Im\phi_1^0 \cos \beta + Im\phi_2^0 \sin \beta] \\ A^0 &= \sqrt{2}[-Im\phi_1^0 \sin \beta + Im\phi_2^0 \cos \beta], \end{aligned} \quad (3.17)$$

The would-be Goldstone bosons G^\pm and G^0 are eaten by the W and Z bosons. The physical Higgs boson masses are

$$m_{H^\pm}^2 = \lambda_4 v^2, \quad (3.18)$$

$$m_{A^0}^2 = \lambda_6 v^2, \quad (3.19)$$

where $v^2 = v_1^2 + v_2^2$ is fixed by the W boson mass, $M_W^2 = \frac{1}{2}g^2 v^2$. Diagonalizing the mass matrix of CP-even Higgs

$$v^2 \begin{pmatrix} 4\cos^2 \beta (\lambda_1 + \lambda_3) + \sin^2 \beta \lambda_5 & (4\lambda_3 + \lambda_5) \sin 2\beta / 2 \\ (4\lambda_3 + \lambda_5) \sin 2\beta / 2 & 4\sin^2 \beta (\lambda_2 + \lambda_3) + \cos^2 \beta \lambda_5 \end{pmatrix}, \quad (3.20)$$

results in the CP-even eigenstates

$$\begin{aligned} H^0 &= \sqrt{2}[(Re\phi_1^0 - v_1) \cos \alpha + (Re\phi_2^0 - v_2) \sin \alpha], \\ h^0 &= \sqrt{2}[(-Re\phi_1^0 - v_1) \sin \alpha + (Re\phi_2^0 - v_2) \cos \alpha] \end{aligned} \quad (3.21)$$

with masses

$$m_{h^0}^2 + m_{H^0}^2 = v^2[4(\cos^2 \beta \lambda_1 + \sin^2 \beta \lambda_2) + \lambda_+], \quad (3.22)$$

$$m_{H^0}^2 - m_{h^0}^2 = v^2[\lambda_- \cos 2\beta - 4\lambda_2 \sin^2 \beta + 4\lambda_1 \cos^2 \beta] / \cos 2\alpha \quad (3.23)$$

and mixing angle

$$\tan 2\alpha = \frac{\lambda_+ \sin 2\beta}{\lambda_- \cos 2\beta - 4\lambda_2 \sin^2 \beta + 4\lambda_1 \cos^2 \beta} \quad (3.24)$$

where $\lambda_\pm = 4\lambda_3 \pm \lambda_5$. In the potential (3.14) there are 8 parameters : λ_i , $i=1, \dots, 6$, v_1 and v_2 . Because, as said above, v^2 is fixed by m_W , there are seven independent parameters in a general CP

invariant 2HDM. Six of them can be expressed in terms of mixing angles α and β and Higgs masses $m_{H^\pm}, m_{A^0}, m_{H^0}, m_{h^0}$. The seventh needs to be fixed by measuring one of the quartic coupling in (3.14). For simplicity we shall assume $\lambda_1 = \lambda_2$ hereafter so that we have six independent parameters in the model. Taking $\lambda_1 = \lambda_2$, eqs.(3.22, 3.23, 3.24) reduce to

$$m_{H^0}^2 + m_{h^0}^2 = v^2(4\lambda_1 + \lambda_+) , \quad (3.25)$$

$$m_{H^0}^2 - m_{h^0}^2 = v^2 \sqrt{(4\lambda_1 + \lambda_-)^2 \cos^2 2\beta + \lambda_+^2 \sin^2 2\beta} \quad (3.26)$$

$$\tan 2\alpha = \frac{\lambda_+}{\lambda_- + 4\lambda_1} \tan 2\beta. \quad (3.27)$$

The three equations show explicitly that the angle α as well as masses m_{H^0}, m_{h^0} can be traded for λ_i , $i=1,3,5$ (or, equivalently, $1,+, -$) no matter how large $\tan\beta$ is. That is, α , as one of the set of six independent parameters which contains both α and β as well as others, can take any value independent of $\tan\beta$, as it should be. Therefore, the statement in ref. [9] that the angle α depends on β is not correct. When $\tan\beta$ approaches to infinity, if $(4\lambda_1 + \lambda_-)$ and consequently $m_{H^0}^2 - m_{h^0}^2$ is of order $\cot\beta$, say, $(4\lambda_1 + \lambda_-) = c \tan 2\beta$ with c a constant of order one., then $\sin 2\alpha$ is of order one. If $(4\lambda_1 + \lambda_-)$ is of order one, then in the large $\tan\beta$ limit it follows that $\sin\alpha \sim \cot\beta$ or $1 - \cot^2\beta / 2$ so that $\sin 2\alpha$ goes always as $\cot\beta$ which cancels the $\tan\beta$ enhancement. However, the conclusion is valid only at tree level. Once the radiative corrections are included it would change, which is similar to the situation that happens in the Higgs sector of MSSM, i.e., the radiative corrections violate the tree level mass relations and one treats Higgs boson masses as free parameters to be determined by experiments. Therefore, even in this case we should still treat α as well as β and Higgs masses as free parameters in the general 2HDM defined above so that the $\tan^2\beta$ enhancement due to the trilinear $H^\pm H^\mp H$ ($H=h^0, H^0$) couplings should be considered, as we did in ref. [5].

As usual, in the model II 2HDM the Higgs–fermion Yukawa couplings are given by

$$L_{Yuk} = -Y_D \bar{Q} \Phi_1 D - Y_U \bar{Q} \Phi_2^c U - Y_l \bar{L} \Phi_1 l + \text{h.c.} \quad (3.28)$$

where $\Phi^c = i\tau_2 \Phi^*$. So down–type quarks and charged leptons (up–type quarks) acquire masses by their couplings to Φ_1 (Φ_2).

Feynman rules in the above general 2HDM have been given. Vertices with one or two gauge bosons and vertices involving two fermions and one boson are given in ref. [18]. The three Higgs boson vertices can be found in ref. [4]. The vertices involving one Goldstone boson and two Higgs bosons have also been given in ref. [18]. We use these Feynman rules in calculations of Wilson coefficients.

As pointed out in section II, for large $\tan\beta$, $C_9(m_W)$ in the 2HDM is the same as that in SM. The leading contributions to C_{Q_i} in the large $\tan\beta$ limit come from the diagrams in Fig. 1. In our previous paper [5] we paid attention to the contributions of neutral Higgs bosons and missed the contribution from the box diagram involving one charged Higgs and one W boson which is of order $\tan^2\beta$ in the large $\tan\beta$ limit [9]. We carry out a calculation for the diagram and confirm the result in ref. [9]. In this paper we include the contribution and correct a sign for A^0 penguin. In order to separate contributions from individual diagrams, we write C_{Q_i} as

$$C_{Q_i} = C_{Q_i}^S + C_{Q_i}^B + C_{Q_i}^P, \quad (3.29)$$

where $C_{Q_i}^S$, $C_{Q_i}^B$, and $C_{Q_i}^P$ denote the contributions from self-energy type diagrams, box diagrams, and Higgs penguin diagrams, respectively. In appendix A we present all contributions proportional to $\tan^2\beta$ in Feynman-t'Hooft gauge. Adding all $\tan^2\beta$ contributions together, we have

$$C_{Q_1}(m_W) = f_{ac}y_t \left[\frac{\ln y_t}{1-y_t} - \frac{\sin^2(2\alpha)}{4} \frac{(m_{h^0}^2 - m_{H^0}^2)^2}{m_{h^0}^2 m_{H^0}^2} f_1(y_t) \right], \quad (3.30)$$

$$C_{Q_2}(m_W) = -f_{ac}y_t \frac{\ln y_t}{1-y_t}. \quad (3.31)$$

$$C_{Q_3}(m_W) = \frac{m_b e^2}{m_\tau g^2} (C_{Q_1}(m_W) + C_{Q_2}(m_W)), \quad (3.32)$$

$$C_{Q_4}(m_W) = \frac{m_b e^2}{m_\tau g^2} (C_{Q_1}(m_W) - C_{Q_2}(m_W)), \quad (3.33)$$

$$C_{Q_i}(m_W) = 0, \quad i = 5, \dots, 10 \quad (3.34)$$

where

$$f_{ac} = \frac{m_b m_t \tan^2\beta}{4 \sin^2\theta_W m_W^2}, \quad x_t = \frac{m_t^2}{m_W^2}, \quad y_t = \frac{m_t^2}{m_{H^\pm}^2}, \quad f_1(y) = \frac{1-y+y \ln y}{(y-1)^2}.$$

The difference between eq.(3.30) and the result in ref. [9] is that the first term in the brackets in eq.(3.30) is incorrectly omitted in ref. [9]. It is worth to note that in the above equations $m_b = m_b(m_W)$.

3.2 In SUSY

In the minimal supersymmetric standard model (MSSM) or supergravity model (SUGRA) the Higgs sector is the same as that in a model II 2HDM by imposing the following constraints on the parameters [18]:

$$\lambda_2 = \lambda_1 \quad (3.35)$$

$$\lambda_3 = \frac{1}{8}(g^2 + g'^2) - \lambda_1 \quad (3.36)$$

$$\lambda_4 = 2\lambda_1 - \frac{1}{2}g'^2 \quad (3.37)$$

$$\lambda_5 = \lambda_6 = -2(\lambda_1 + 2\lambda_3). \quad (3.38)$$

And all Feynman rules can be found in ref. [18]. In addition to Fig. 1, the diagrams in Fig. 2 also give the leading contributions. Besides box diagrams, five different sets of contributions to the decay $b \rightarrow sl^+l^-$ are present in SUSY. They can be classified according to the virtual particles exchanged in the loop: *a*) the SM contribution with exchange of W^- and up-quarks; *b*) the charged Higgs boson contribution with H^- and up-quarks; *c*) the chargino contribution with χ^- and up-squarks (\tilde{u}); *d*) the gluino contribution with \tilde{g} and down-squarks (\tilde{d}); and finally *e*) the neutralino contribution with χ^0 and down-squarks. As pointed out in refs. [14, 15, 7], contributions from neutrino-down type squark (*e*) and gluino-down type squark (*d*) loop diagrams are negligible compared to those from

chargino-up type squark diagrams because the flavor mixings between the third and the other two generations are small in minimal supergravity and constrained MSSM. Therefore, in addition to the SM (a) and charged Higgs (b) contributions, we only include the contributions from chargino-up type squark (c) loop diagrams in the paper.

In some regions of the parameter space the dominant contribution to C_{Q_i} is proportional to $\tan^3\beta$ and comes from the self-energy type diagrams, as pointed out in ref. [6, 7, 19]. In quite a large region of the parameter space the dominant contribution is proportional to $\tan^2\beta$. Box diagrams can contribute terms with $\tan^4\beta$ to C_{Q_i} which are greatly suppressed by $(m_s/M_W)^2$, therefore the largest contributions to C_{Q_i} from SUSY box diagrams remain proportional to $\tan^2\beta$. Among the diagrams in Fig.2 only the box diagram with charginos in the loop can give the $\tan^2\beta$ enhancement to $C_9(m_W)$. The contributions of the self energy type and penguin diagrams to C_{Q_i} have been calculated by us in refs. [6, 7]. We calculate the contributions of the box diagrams and summarize all contributions in the appendix B. Adding all contributions given in the appendix B, one has

$$\begin{aligned}
C_{Q_1}(M_W) = & f_{ac} \left\{ -\frac{\sin^2(2\alpha)}{2} \frac{(m_{h^0}^2 - m_{H^0}^2)^2}{2m_{h^0}^2 m_{H^0}^2} y_t f_1(y_t) - (x_t - 1) f_{C^0}(x_{H^-}, 1, x_t) \right. \\
& - f_{C^0}(x_{H^-}, 1, 0) \left. \right\} - f_{ac} \frac{M_W}{m_b \lambda_t} \sum_{i,j=1}^2 \sum_{k,k'=1}^6 \mathcal{H}_{j b k'} \Gamma_{i s k}^\dagger \left\{ \delta_{ij} \delta_{k k'} r_{hH} \sqrt{x_{\chi_i^-}} f_{B^0}(x_{\chi_i^-}, x_{\tilde{u}_k}) \right. \\
& - \frac{\sqrt{2}}{\tan\beta} [\delta_{k k'} G_{ijk}^{hH} f_{C^0}(x_{\chi_i^-}, x_{\chi_j^-}, x_{\tilde{u}_k}) + \delta_{ij} F_{k k'}^{hH} \sqrt{x_{\chi_i^-}} f_{C^0}(x_{\chi_i^-}, x_{\tilde{u}_k}, x_{\tilde{u}_{k'}})] \\
& \left. + \frac{1}{\tan\beta} \delta_{k k'} \left(\sqrt{x_{\chi_i^-} x_{\chi_j^-}} Q_{ij} + x_{\tilde{u}_k} Q_{ij}^\dagger \right) f_{D^0}(x_{\chi_i^-}, x_{\chi_j^-}, x_{\tilde{u}_k}, x_{\tilde{\nu}_l}) \right\} \quad (3.39)
\end{aligned}$$

$$\begin{aligned}
= & -\tan^3\beta \frac{m_b m_\ell}{4 \sin^2\theta_w M_W^2 \lambda_t} \sum_{i=1}^2 \sum_{k=1}^6 U_{i2} T_{UL}^{km} K_{mb} \{ -\sqrt{2} V_{i1} (T_{UL} K)_{ks}^* + V_{i2} \frac{(T_{UR} \tilde{m}_u K)_{ks}^*}{M_W \sin\beta} \} \\
& r_{hH} \sqrt{x_{\chi_i^-}} f_{B^0}(x_{\chi_i^-}, x_{\tilde{u}_k}) + O(\tan^2\beta), \quad (3.40)
\end{aligned}$$

$$\begin{aligned}
C_{Q_2}(M_W) = & f_{ac} \left[(x_t - 1) f_{C^0}(x_{H^-}, 1, x_t) + f_{C^0}(x_{H^-}, 1, 0) \right] \\
& + f_{ac} \frac{M_W}{m_b \lambda_t} \sum_{i,j=1}^2 \sum_{k,k'=1}^6 \mathcal{H}_{j b k'} \Gamma_{i s k}^\dagger \left\{ \delta_{ij} \delta_{k k'} r_A \sqrt{x_{\chi_i^-}} f_{B^0}(x_{\chi_i^-}, x_{\tilde{u}_k}) \right. \\
& + \frac{\sqrt{2}}{\tan\beta} [\delta_{k k'} G_{ijk}^A f_{C^0}(x_{\chi_i^-}, x_{\chi_j^-}, x_{\tilde{u}_k}) + \delta_{ij} F_{k k'}^A \sqrt{x_{\chi_i^-}} f_{C^0}(x_{\chi_i^-}, x_{\tilde{u}_k}, x_{\tilde{u}_{k'}})] \\
& \left. - \frac{1}{\tan\beta} \delta_{k k'} \left(\sqrt{x_{\chi_i^-} x_{\chi_j^-}} Q_{ij} - x_{\tilde{u}_k} Q_{ij}^\dagger \right) f_{D^0}(x_{\chi_i^-}, x_{\chi_j^-}, x_{\tilde{u}_k}, x_{\tilde{\nu}_l}) \right\} \quad (3.41)
\end{aligned}$$

$$= \tan^3\beta \frac{m_b m_\ell}{4 \sin^2\theta_w M_W^2 \lambda_t} \sum_{i=1}^2 \sum_{k=1}^6 U_{i2} T_{UL}^{km} K_{mb} \{ -\sqrt{2} V_{i1} (T_{UL} K)_{ks}^* + V_{i2} \frac{(T_{UR} \tilde{m}_u K)_{ks}^*}{M_W \sin\beta} \}$$

$$r_A \sqrt{x_{\chi_i^-}} f_{B^0}(x_{\chi_i^-}, x_{\tilde{u}_k}) + O(\tan^2 \beta), \quad (3.42)$$

$$\begin{aligned} C_9(M_W) = & -\frac{1}{4\sin^2 \theta_W} \left\{ x_t F_9(x_t) - G(x_t, 0) + G(0, 0) + \frac{y_t}{2} ctg^2 \beta \left(F_2(y_t) + F_4(y_t) \right) \right. \\ & - \sum_{i,j=1}^2 \sum_{k,k'=1}^6 \Gamma_{jbk'} \Gamma_{isk}^\dagger \left[\frac{1}{4} \left(\delta_{ij} \sum_{m=1}^3 T_{UL}^{km} T_{UL}^{\dagger mk'} G_0(x_{\tilde{u}_k \chi_j^-}, x_{\tilde{u}_{k'} \chi_j^-}) \right. \right. \\ & + 2\delta_{kk'} \sqrt{x_{\chi_j^-} \tilde{u}_{k'}} x_{\chi_i^- \tilde{u}_k} U_{j1}^* U_{i1} F_0(x_{\chi_j^- \tilde{u}_k}, x_{\chi_i^- \tilde{u}_k}) - \delta_{kk'} V_{j1} V_{i1}^* \left[\log(x_{\tilde{u}_k}) + G_0(x_{\chi_j^- \tilde{u}_k}, x_{\chi_i^- \tilde{u}_k}) \right] \Big) \\ & \left. - \frac{1}{2} \delta_{kk'} \left(\frac{1}{x_{\chi_j^-}} V_{j1} V_{i1}^* G'(x_{\tilde{u}_k \chi_j^-}, x_{\tilde{\nu}_\tau \chi_j^-}, x_{\chi_i^- \chi_j^-}) \right) \right. \\ & \left. \left. + \frac{m_\ell^2}{M_W^2} \tan^2 \beta \sqrt{x_{\chi_j^-} x_{\chi_i^-}} U_{j2}^* U_{i2} f_{D^0}(x_{\chi_i^-}, x_{\chi_j^-}, x_{\tilde{u}_k}, x_{\tilde{\nu}_l}) \right) \right] \Big\}, \end{aligned} \quad (3.43)$$

where U and V are matrices which diagonalize the mass matrix of charginos, T_{Ui} ($i=L, R$) is the matrix which diagonalizes the mass matrix of the scalar up-type quarks and K is the CKM matrix. For the definitions of various symbols in the above equations, see the Appendix B. In eqs. (3.40) and (3.42) the $\tan^3 \beta$ term has been explicitly written.

Let us give some remarks:

(a) The first term in eq. (3.39) which is proportional to $\sin^2 2\alpha$ arises from the trilinear $H^\pm H^\mp H$ couplings. At tree level, due to the more constraints (3.36-3.38) than that in the 2HDM defined in subsection 3.1, there are only two free parameters in the Higgs sector of MSSM which we may choose as $\tan \beta$ and one of masses of Higgs bosons, e. g., m_{A^0} . In the large $\tan \beta$ limit one has

$$\begin{aligned} m_{h^0}^2 &\approx m_Z^2, & m_{H^0} &\approx m_{A^0}, & m_{H^\pm}^2 &= m_{A^0}^2 + m_W^2, \\ \sin 2\alpha &\sim \cot \beta. \end{aligned} \quad (3.44)$$

So the first term would have no $\tan \beta$ enhancement. However, including the radiative corrections, the above relations are, in general, changed and the mixing angle α is determined by

$$\tan 2\alpha = \frac{\sin 2\beta (m_{A^0}^2 + m_Z^2) - 2R_{12}}{\cos 2\beta (m_{A^0}^2 - m_Z^2) + R_{22} - R_{11}}, \quad -\frac{\pi}{2} < \alpha \leq 0, \quad (3.45)$$

where R_{ij} are the radiative corrections to the mass matrix of the neutral Higgs bosons in the $\{H_1^0, H_2^0\}$ basis and have been given in refs.[20, 21]. As shown in ref.[22], R_{12} can reach more than ten percents of R_{22} in the case of $\mu \sim A_t \sim A_b$ and consequently $\sin 2\alpha$ can be the order of one. Of course, there are some cases in which R_{12} as well as R_{11} is very small and of a few thousandth of R_{22} and consequently the tree level relations (3.44) are almost not changed. Therefore, we keep, in general, α and Higgs boson masses as free parameters because several parameters in MSSM enter the Higgs sector through the radiative corrections.

(b) The first terms in eqs. (3.40, 3.42) which arise from the self-energy type diagram will provide the $\tan^3 \beta$ enhancement, as pointed out in [6, 7], if the mass splittings of stops are large (say, $\geq 100 \text{ GeV}$). The condition is necessary because if all the squark masses are degenerate ($m_{\tilde{t}_1} = m_{\tilde{t}_2} =$

m_b	m_c	m_μ	m_τ	M_{B_s}	f_{B_s}	G_F
4.8 GeV	1.4 GeV	0.11 GeV	1.78 GeV	5.37 GeV	0.22 GeV	$1.17 \times 10^{-5} \text{GeV}^{-2}$
α^{-1}	$ V_{ts}^* V_{tb} $	$ V_{cb} $	$Br(b \rightarrow c e \nu_e)$	τ_{B_s}	$\sin^2 \theta_w$	$\alpha_s(M_z)$
129	0.0385	0.036	0.114	$1.54 \times 10^{-12} \text{s}$	0.232	0.12

Table 1: *Values of the standard model parameters used in our numerical analysis.*

α	m_{h^0}	m_{H^0}	m_{A^0}	m_{H^\pm}	$m_{\chi_1^-}$	$m_{\tilde{\nu}_\tau}$
0.08	110 GeV	160 GeV	160 GeV	180 GeV	90 GeV	150 GeV

Table 2:

\tilde{m}), the large contributions arising from the chargino-squark loop exactly cancel due to the GIM mechanism[23]. We remark that the chirality structure of the Q_i ($i=1, 2$) operators allows a large $\tan\beta$ enhancement for the Wilson coefficients C_{Q_i} ($i=1, 2$), as happened for the magnetic moment operator O_7 , and there is no such a large $\tan\beta$ enhancement for the Wilson coefficients C_i ($i=8, 9$) due to the different chirality structure of the O_i ($i=8, 9$) operators.

(c)The last term in eq. (3.43) comes from the chargino-chargino box diagrams and are proportional to $\tan^2\beta$. It was missed in the literature. For $l=\mu, \tau$ and large $\tan\beta$, it is numerically the same size as the other contributions so that it should not be omitted.

4 Numerical results

Below we assume no CP violating phases from 2HDM and SUSY. As said in section II, there are 6 free parameters in the 2HDM which are $\tan\beta$, α , m_{h^0} , m_{H^0} , m_{A^0} , m_{H^\pm} . In MSSM, in addition to the above 6 parameters, 7 extra free parameters, $m_{\tilde{c}_L}$, $m_{\tilde{t}_L}$, $m_{\tilde{t}_R}$, A_t , M_2 , μ , and $m_{\tilde{\nu}_\tau}$ are needed in order to calculate the Wilson coefficients. In Table. 1 we list all SM inputs for our numerical analysis.

Numerical results are given in Figs. 3-9. Figs. 3-5 are devoted to the decay $B_s \rightarrow \mu^+\mu^-$ in 2HDM. In the numerical calculations in 2HDM the constraint on m_{H^\pm} from $b \rightarrow s\gamma$ [25] has been imposed. We present in Fig. 3 the branching ratio (Br) for $B_s \rightarrow \mu^+\mu^-$ as the function of m_{H^0} , the mass of the heavier CP even neutral Higgs boson, for fixed values of the other parameters. The figure shows that the Br increases when m_{H^0} increases except for the mixing angle $\alpha=0$. The reason is that in the large $\tan\beta$ case the trilinear $H^\pm H^\mp H$ ($H=H^0, h^0$) couplings are proportional to $m_{H^0}^2$ and/or $m_{h^0}^2$ and the couplings vanish when α is equal to zero. One can see from Fig. 4 that the Br, as the function of α , behaves like $\sin^2 2\alpha$ when m_{H^0} is large enough (say, 500 GeV), which implies the contributions from the trilinear couplings of NHBs dominate (see eqs. (2.13), (3.30) and (3.31)). Fig. 5 shows the $\tan\beta$ dependence of Br and one can see from it that the contributions coming from C_{Q_i} 's can dominate when $\tan\beta$ is large enough (say, larger than 80). In most of the large $\tan\beta$ region in the parameter space Br is of order 10^{-8} , an order of magnitude larger than that in SM.

The numerical results in MSSM are presented in Figs. 6-9. We present the correlation between C_7 and C_{Q_1} for $l = \mu$ and $l = \tau$ respectively in Fig. 6 and 7 where the absolute values of C_7 are

taken from the data of $B \rightarrow X_s \gamma$ [25] with the 2σ errors imposed. We set $m_{\tilde{t}_1}$, $m_{\tilde{t}_2}$, $m_{\tilde{c}_L}$, $m_{\chi_2^-}$, and $\tan\beta$ as random free parameters. They vary in the range 180-300 GeV, 250-450 GeV, 200-400 GeV, 160-360 GeV and 25-50 respectively. Other parameters are fixed as given in Table 2. We get about 3000 permitted points among 25000 points. The contributions to Wilson coefficients due to superparticles in a loop (SUSY contributions) come mainly through the $\tilde{u}_k^* \bar{\chi}_i d$ vertex, which is determined by the mixing between Higgsinos and Winos and the mixing between stops. The vertex appears in Feynman diagrams which describe the processes $b \rightarrow s \gamma$ and $b \rightarrow s l^+ l^-$ so that there exists a correlation between C_7 and C_{Q_i} . In some large $\tan\beta$ regions of the parameter space in MSSM, SUSY contributions interfere destructively with the SM contributions and SUSY contributions can be so large that they can overwhelm those from the SM and the Higgs sector so that the sign of C_7 is changed compared to that in SM, as shown in Fig. 6 and 7. In the regions C_{Q_i} s are proportional to $\tan^3\beta$ and consequently can compete with C_9 for $l=\mu$ and be much larger than C_9 for $l=\tau$. We also calculate the correlation between C_{Q_1} and C_{Q_2} in the regions and it follows that $C_{Q_1} \approx -C_{Q_2}$.

The contribution to C_9 which is proportional to $\tan^2\beta$ coming from chargino-chargino box diagrams is numerically the same order as other contributions from chargino-chargino box or chargino-up type squark penguin diagrams. As a whole SUSY contributions to C_9 give about 10% corrections to the SM value. Taking C_{Q_1} in the allowed range in Figs. 6 and 7 and $C_{Q_2} \approx -C_{Q_1}$, we draw the branching ratio of $B_s \rightarrow l^+ l^-$ as function of C_{Q_1} in Figs. 8 and 9, given C_9 being the SM value with 10% variations. Figs. 8 is for $l=\mu$ and Fig. 9 for $l=\tau$. From Figs. 8,9, we can see that $\text{Br}(B_s \rightarrow l^+ l^-)$ is more sensitive to C_{Q_i} 's (which represent the contributions from NHBs) than to C_9 in the large $\tan\beta$ (larger than about 30) regions because in the regions $|C_{Q_i}'|$ s are much larger than $|\frac{m_l}{m_{B_s}} C_9|$. The numerical results tell us that it is possible to saturate the experimental bound (1.1) for $B_s \rightarrow \mu^+ \mu^-$ in some regions of the parameter space in MSSM. In other words, the experimental bound could impose a constraint on the parameter space of SUSY which we shall analyze elsewhere. Because C_{Q_i} 's are proportional to the lepton mass, Br for $l=\tau$ can reach order of 10^{-4} in the regions in which $\text{Br}(B_s \rightarrow \mu^+ \mu^-)$ saturates the experimental bound.

5 Conclusions

In summary we have analyzed the decays $B_s \rightarrow \ell^+ \ell^-$ in the model II 2HDM and SUSY with large $\tan\beta$. Although these decays have been studied in these models before and reanalyzed recently, it seems that no complete analysis exists so far. We have calculated all leading terms in the large $\tan\beta$ limit. We found that in addition to the Higgs boson-W boson box diagram, the chargino-chargino box diagram gives also a contribution proportional to $\tan^2\beta$, the former to C_{Q_i} ($i=1,2$) and the latter to C_i ($i=8,9$). The contributions from NHBs always increase the branching ratios in the large $\tan\beta$ case so that the branching ratios in the 2HDM and in SUSY are larger than those in SM. We have numerically computed the branching ratios for $l=\mu$ and τ . In the 2HDM the branching ratio for $l=\mu$ is about 10^{-8} , an order of magnitude larger than that in SM, if $\tan\beta = 50$ or so and the other parameters are in the reasonable range. We have shown the dependence of the branching ratio with respect to the mixing angle α and neutral Higgs boson masses. The branching ratio increases when the splitting of the masses of the two CP even neutral Higgs bosons increases except for the case of the mixing angle $\alpha=0$. In MSSM the branching ratio for $l=\mu$ can saturate the experimental bound in some regions of the parameter space where C_{Q_i} s ($i=1,2$) behave as $\tan^3\beta$. In the other regions where C_{Q_i} s ($i=1,2$) behave as $\tan^2\beta$ the branching ratio is about the order 10^{-8} . The branching

ratio for $l=\tau$ reaches 10^{-4} in the regions of the parameter space in which $\text{Br}(B_s \rightarrow l^+l^-)$ saturates the experimental bound. In the near future when very high statistics can be reached [2, 24] the measurements of the decays $B_s \rightarrow l^+l^-$ ($l=\mu, \tau$) can provide a large potential to find or exclude the large $\tan\beta$ parts of the parameter space in 2HDM and/or SUSY.

Acknowledgements

One of the authors (C.-S. Huang) would like to thank Gad Eilam for discussions and Department of Physics, Technion-Israel Institute of Technology where a part of work was done for warm hospitality. This work was supported in part by the National Nature Science Foundation of China and supported in part by the Alexander von Humboldt Foundation.

Appendix

A Wilson coefficients in a model II 2HDM

Wilson coefficients are extracted from the transition amplitudes by integrating out heavy particles. In our convention, the effective Hamiltonian is related with the amplitude by

$$iM(b \rightarrow sl^+l^-) = -i \langle l^+l^- s | H_{eff} | b \rangle \quad (5.46)$$

By computating the self-energy type, Higgs-penguin and box diagrams, $C_{Q_1}^i$ and $C_{Q_2}^i$ with the superscript denoting the type of a diagram are extracted out, as given below

$$C_{Q_1}^S = f_{ac} r_{hH} (x_{H^-} - 1) x_t f_2(x_t, y_t) , \quad (5.47)$$

$$C_{Q_2}^S = -f_{ac} r_A (x_{H^-} - 1) x_t f_2(x_t, y_t) , \quad (5.48)$$

$$C_{Q_1}^P = -f_{ac} \frac{\sin^2 2\alpha (m_{h^0}^2 - m_{H^0}^2)^2}{2 m_{h^0}^2 m_{H^0}^2} y_t f_1(y_t) \\ - f_{ac} [-1 + (x_{H^-} - 1) r_{hH}] x_t f_2(x_t, y_t) , \quad (5.49)$$

$$C_{Q_2}^P = f_{ac} [-1 + (x_{H^-} - 1) r_A] x_t f_2(x_t, y_t) , \quad (5.50)$$

$$C_{Q_1}^B = -f_{ac} B_+(x_{H^+}, x_t) , \quad (5.51)$$

$$C_{Q_2}^B = f_{ac} B_+(x_{H^+}, x_t) , \quad (5.52)$$

where

$$f_{ac} = \frac{1}{4 \sin^2 \theta_w} \frac{m_b m_\ell}{M_W^2} \tan^2 \beta , r_{hH} = M_W^2 \left(\frac{\sin^2 \alpha}{M_{h^0}^2} + \frac{\cos^2 \alpha}{M_{H^0}^2} \right) , \quad (5.53)$$

$$r_A = \frac{M_W^2}{m_{A^0}^2} , x_{H^-} = \frac{m_{H^-}^2}{M_W^2} , x_t = \frac{m_t^2}{M_W^2} , y_t = \frac{m_t^2}{m_{H^-}^2} , \quad (5.54)$$

$$f_1(y) = \frac{1 - y + y \ln y}{(y - 1)^2}, \quad (5.55)$$

$$f_2(x, y) = \frac{x \ln y}{(z - x)(x - 1)} + \frac{\ln z}{(z - 1)(x - 1)}, \quad \text{with } z = x/y, \quad (5.56)$$

$$B_+(x, y) = \frac{y}{x - y} \left(\frac{\ln y}{y - 1} - \frac{\ln x}{x - 1} \right), \quad (5.57)$$

B Wilson coefficients in MSSM

B.1 Feynman rules and conventions

In this subsection we present our convention. In order to avoid the trouble in dealing with charge conjugate operation, we choose χ^- as the particle. The interactions of $d\tilde{u}\chi$, $H\chi\chi$, $H\tilde{u}\tilde{u}$, and Hdd can be expressed as:

$$\mathcal{L}_{d\tilde{u}\chi} = \frac{g_2}{\sqrt{2}} \tilde{u}_k^* \bar{\chi}_i^- [\Gamma_{ijk} P_L + \mathcal{H}_{ijk} P_R] d_j + h.c. , \quad (5.58)$$

$$\mathcal{L}_{H\chi\chi} = \frac{g_2}{\sqrt{2}} \bar{\chi}_i^- [g_{ijh}^- P_L + g_{ijh}^+ P_R] \chi_j^- H_h^0 + h.c. , \quad (5.59)$$

$$\mathcal{L}_{H\tilde{u}\tilde{u}} = \frac{g_2}{\sqrt{2}} f_{ijh} \tilde{u}_i^* \tilde{u}_j H_h^0 + h.c. , \quad (5.60)$$

$$\mathcal{L}_{Hdd} = \frac{g_2}{\sqrt{2}} g_h \bar{d} d H_h^0 , \quad (5.61)$$

where

$$\Gamma_{ijk} = -\sqrt{2} V_{i1}^* (T_{UL} K)_{kj} + V_{i2}^* \frac{(T_{UR} \tilde{m}_u K)_{kj}}{M_W \sin \beta} , \quad (5.62)$$

$$\mathcal{H}_{ijk} = U_{i2} \frac{(T_{UL} K \tilde{m}_d)_{kj}}{M_W \cos \beta} , \quad (5.63)$$

$$g_{ijh}^+ = \sqrt{2} \{ (Q_{ij} \sin \alpha - S_{ij} \cos \alpha), -(Q_{ij} \cos \alpha + S_{ij} \sin \alpha), -i(Q_{ij} \sin \beta + S_{ij} \cos \beta) \}_h , \quad (5.64)$$

$$g_{ijh}^- = \sqrt{2} \{ (Q_{ij}^\dagger \sin \alpha - S_{ij}^\dagger \cos \alpha), -(Q_{ij}^\dagger \cos \alpha + S_{ij}^\dagger \sin \alpha), i(Q_{ij}^\dagger \sin \beta + S_{ij}^\dagger \cos \beta) \}_h , \quad (5.65)$$

$$g_h = \frac{m_d}{\sqrt{2} M_W} \left\{ \frac{\sin \alpha}{\cos \beta}, -\frac{\cos \alpha}{\cos \beta}, i \tan \beta \gamma_5 \right\}_h , \quad (5.66)$$

$$f_{ijh} = T_{il} H_{ll'}^h T_{l'j}^\dagger, Q_{ij} = \frac{1}{\sqrt{2}} U_{i2} V_{j1}, S_{ij} = \frac{1}{\sqrt{2}} U_{i1} V_{j2} . \quad (5.67)$$

In (7.58) and (7.59) K is the CKM matrix, and \tilde{m}_u and \tilde{m}_d are defined as

$$\tilde{m}_u = \text{diag}\{m_u, m_c, m_t\}, \tilde{m}_d = \text{diag}\{m_d, m_s, m_b\} . \quad (5.68)$$

H^h can be expressed as

$$H^{h0} = - \begin{pmatrix} \sqrt{2} \left[\frac{\cos\alpha}{\sin\beta} \frac{\tilde{m}_u^2}{M_W} - \frac{\sin(\alpha+\beta)}{\cos^2\theta_w} D_{uL} M_W \right] & \frac{\tilde{m}_u}{\sqrt{2}M_W} \left(\frac{\sin\alpha}{\sin\beta} \mu 1 + \frac{\cos\alpha}{\sin\beta} A^\dagger \right) \\ \frac{1}{\sqrt{2}M_W} \left(\frac{\sin\alpha}{\sin\beta} \mu^* 1 + \frac{\cos\alpha}{\sin\beta} A \right) \tilde{m}_u & \sqrt{2} \left[\frac{\cos\alpha}{\sin\beta} \frac{\tilde{m}_u^2}{M_W} - \frac{\sin(\alpha+\beta)}{\cos^2\theta_w} D_{uR} M_W \right] \end{pmatrix}, \quad (5.69)$$

$$H^{H0} = - \begin{pmatrix} \sqrt{2} \left[\frac{\sin\alpha}{\sin\beta} \frac{\tilde{m}_u^2}{M_W} + \frac{\cos(\alpha+\beta)}{\cos^2\theta_w} D_{uL} M_W \right] & \frac{\tilde{m}_u}{\sqrt{2}M_W} \left(-\frac{\cos\alpha}{\sin\beta} \mu 1 + \frac{\sin\alpha}{\sin\beta} A^\dagger \right) \\ \frac{1}{\sqrt{2}M_W} \left(-\frac{\cos\alpha}{\sin\beta} \mu^* 1 + \frac{\sin\alpha}{\sin\beta} A \right) \tilde{m}_u & \sqrt{2} \left[\frac{\sin\alpha}{\sin\beta} \frac{\tilde{m}_u^2}{M_W} + \frac{\cos(\alpha+\beta)}{\cos^2\theta_w} D_{uR} M_W \right] \end{pmatrix}, \quad (5.70)$$

$$H^{A0} = - \begin{pmatrix} 0 & \frac{-i\tilde{m}_u}{\sqrt{2}M_W} (\mu 1 + ctg\beta A^\dagger) \\ \frac{i}{\sqrt{2}M_W} (\mu^* 1 + Actg\beta) \tilde{m}_u & 0 \end{pmatrix}. \quad (5.71)$$

where

$$D_{uL} = \left(\frac{1}{2} - e_u \sin^2\theta_w \right), D_{uR} = e_u \sin^2\theta_w. \quad (5.72)$$

The 6×6 mass matrix of u-type squark is given as

$$\mathcal{M}_{\tilde{u}} = \begin{pmatrix} (m_{\tilde{Q}}^2 + \tilde{m}_u^2) + \cos 2\beta D_{uL} m_z^2 & \tilde{m}_u (-\mu ctg\beta 1 + A^\dagger) \\ (-\mu^* ctg\beta 1 + A) \tilde{m}_u & m_{\tilde{U}}^2 + \tilde{m}_u^2 + \cos 2\beta D_{uR} m_z^2 \end{pmatrix}, \quad (5.73)$$

where each block is a 3×3 matrix. A is defined by $Y^u = Ah^u$, while Y^u is the trilinear coupling matrix of up-type squarks, and h^u is the Yukawa coupling of up-type quarks. The 6×6 T matrix is defined as

$$diag m_{\tilde{u}_k}^2 = T \mathcal{M}_{\tilde{u}} T^\dagger, \tilde{u}_k = T_{UL}^{kl} K_{\tilde{u}} \tilde{u}_L^i + T_{UR}^{ki'} \tilde{u}_R^{i'}. \quad (5.74)$$

The convention of chargino masses is given as

$$\mathcal{L}_{\chi\chi} = -\phi^{-T} X \phi^+ + h.c., \quad (5.75)$$

$$X = \begin{pmatrix} M_2 & \sqrt{2} M_W \sin\beta \\ \sqrt{2} M_W \cos\beta & \mu \end{pmatrix}, \quad (5.76)$$

$$\phi^{-T} = \{-i\lambda^-, \phi_{H_1}^-\}, \phi^{+T} = \{-i\lambda^+, \phi_{H_2}^+\}, \quad (5.77)$$

$$\phi^- = U^+ \chi_0^-, \phi^+ = V^+ \chi_0^+, \chi_i^{-T} = \{\chi_{0i}^-, \bar{\chi}_{0i}^+\}. \quad (5.78)$$

where

$$U^* X V^\dagger = diag\{m_{\chi_1^\pm}, m_{\chi_2^\pm}\} \quad (5.79)$$

With the above conventions, it is straightforward to extract Feynman rules.

B.2 C_9 , C_{Q_1} and C_{Q_2} in SUSY

Wilson coefficients are extracted from the transition amplitudes by integrating out heavy particles. C_9 is given as

$$C_9 = C_{9,z} + C_{9,B} \quad (5.80)$$

$$C_{9,z} = C_{9,z}^W + C_{9,z}^{H^-} + C_{9,z}^{\chi^-} \quad (5.81)$$

$$C_{9,B} = C_{9,B}^W + C_{9,B}^{\chi^-} \quad (5.82)$$

$$C_{9,z}^W = -\frac{x_t}{4\sin^2\theta_W} F_9(x_{tW}) \quad (5.83)$$

$$C_{9,z}^{H^-} = -\frac{x_t}{4\sin^2\theta_W} \frac{x_{th}}{2} ctg^2\beta [F_3(x_{th}) + F_4(x_{th})] \quad (5.84)$$

$$\begin{aligned} C_{9,z}^{\chi^-} = & \frac{1}{4\lambda_t \sin^2\theta_W} \frac{1}{4} \sum_{i,j=1}^2 \sum_{k,k'=1}^6 \Gamma_{j b k'} \Gamma_{i s k}^\dagger \left\{ \delta_{ij} \sum_{m=1}^3 T_{UL}^{km} T_{UL}^{\dagger m k'} G_0(x_{\tilde{u}_k \chi_j}, x_{\tilde{u}_{k'} \chi_j}) \right. \\ & + \delta_{kk'} \left[2\sqrt{x_{\chi_j^-} \tilde{u}_{k'}} x_{\chi_i^- \tilde{u}_k} U_{j1}^* U_{i1} F_0(x_{\chi_j^- \tilde{u}_k}, x_{\chi_i^- \tilde{u}_k}) \right. \\ & \left. \left. + V_{j1} V_{i1}^* \left(-\log(x_{\tilde{u}_k}) - G_0(x_{\chi_j^- \tilde{u}_k}, x_{\chi_i^- \tilde{u}_k}) \right) \right] \right\} \end{aligned} \quad (5.85)$$

$$C_{9,B}^W = \frac{1}{4\sin^2\theta_W} [G(x_{tW}, 0) - G(0, 0)] \quad (5.86)$$

$$\begin{aligned} C_{9,B}^{\chi^-} = & \frac{1}{4\lambda_t \sin^2\theta_W} \frac{1}{2} \sum_{i,j=1}^2 \sum_{k=1}^6 \Gamma_{j b k} \Gamma_{i s k}^\dagger \left[\frac{1}{x_{\chi_j^-}} V_{j1} V_{i1}^* G'(x_{\tilde{u}_k \chi_j^-}, x_{\tilde{\nu}_\tau \chi_j^-}, x_{\chi_i^- \chi_j^-}) \right. \\ & \left. + \frac{m_\ell^2}{M_W^2} \tan^2\beta \sqrt{x_{\chi_j^-} x_{\chi_i^-}} U_{j2}^* U_{i2} f_{D^0}(x_{\chi_i^-}, x_{\chi_j^-}, x_{\tilde{u}_k}, x_{\tilde{\nu}_\tau}) \right] \end{aligned} \quad (5.87)$$

By computing the self energy type, Higgs-penguin and box diagrams, $C_{Q_1}^{ij}$ and $C_{Q_2}^{ij}$ with the first superscript denoting the type of a diagram and the second superscript a Higgs boson or a superparticle in the loop of the diagram are extracted out, as given below

$$C_{Q_{1(2)}}^S = C_{Q_{1(2)}}^{SH} + C_{Q_{1(2)}}^{SS} , \quad (5.88)$$

$$C_{Q_{1(2)}}^P = C_{Q_{1(2)}}^{PH} + C_{Q_{1(2)}}^{PS} , \quad (5.89)$$

$$C_{Q_{1(2)}}^B = C_{Q_{1(2)}}^{BH} + C_{Q_{1(2)}}^{BS} , \quad (5.90)$$

$$C_{Q_1}^{SH} = -f_{ac} r_{hH} (x_{H^-} - 1) x_t f_{C^0}(x_{H^-}, 1, x_t) , \quad (5.91)$$

$$C_{Q_2}^{SH} = f_{ac} r_A (x_{H^-} - 1) x_t f_{C^0}(x_{H^-}, 1, x_t) , \quad (5.92)$$

$$\begin{aligned} C_{Q_1}^{PH} = & -f_{ac} \frac{\sin^2 2\alpha}{2} \frac{(m_{h^0}^2 - m_{H^0}^2)^2}{2m_{H^0}^2 m_{h^0}^2} y_t f_1(y_t) \\ & + f_{ac} [-1 + (x_{H^-} - 1) r_{hH}] x_t f_{C^0}(x_{H^-}, 1, x_t) , \end{aligned} \quad (5.93)$$

$$C_{Q_2}^{PH} = -f_{ac} [-1 + (x_{H^-} - 1) r_A] x_t f_{C^0}(x_{H^-}, 1, x_t) , \quad (5.94)$$

$$C_{Q_1}^{BH} = f_{ac} [f_{C^0}(x_{H^-}, 1, x_t) - f_{C^0}(x_{H^-}, 1, 0)] , \quad (5.95)$$

$$C_{Q_2}^{BH} = -f_{ac} [f_{C^0}(x_{H^-}, 1, x_t) - f_{C^0}(x_{H^-}, 1, 0)] , \quad (5.96)$$

$$C_{Q_1}^{SS} = -f_{ac} r_{hH} \frac{M_W}{m_b \lambda_t} \sum_{i=1}^2 \sum_{k=1}^6 \mathcal{H}_{ibk} \Gamma_{isk}^\dagger \sqrt{x_{\chi_i^-}} f_{B^0}(x_{\chi_i^-}, x_{\tilde{u}_k}) , \quad (5.97)$$

$$C_{Q_2}^{SS} = f_{ac} r_A \frac{M_W}{m_b \lambda_t} \sum_{i=1}^2 \sum_{k=1}^6 \mathcal{H}_{ibk} \Gamma_{isk}^\dagger \sqrt{x_{\chi_i^-}} f_{B^0}(x_{\chi_i^-}, x_{\tilde{u}_k}) , \quad (5.98)$$

$$C_{Q_1}^{PS} = f_{ac} \frac{\sqrt{2} M_W}{m_b \tan \beta \lambda_t} \sum_{i,j=1}^2 \sum_{k,k'=1}^6 \mathcal{H}_{jbb'k'} \Gamma_{isk}^\dagger \left[\delta_{kk'} G_{ijk}^{hH} f_{C^0}(x_{\chi_i^-}, x_{\chi_j^-}, x_{\tilde{u}_k}) \right. \\ \left. + \delta_{ij} F_{kk'}^{hH} \sqrt{x_{\chi_i^-}} f_{C^0}(x_{\chi_i^-}, x_{\tilde{u}_k}, x_{\tilde{u}_{k'}}) \right] , \quad (5.99)$$

$$C_{Q_2}^{PS} = f_{ac} \frac{\sqrt{2} M_W}{m_b \tan \beta \lambda_t} \sum_{i,j=1}^2 \sum_{k,k'=1}^6 \mathcal{H}_{jbb'k'} \Gamma_{isk}^\dagger \left[\delta_{kk'} G_{ijk}^A f_{C^0}(x_{\chi_i^-}, x_{\chi_j^-}, x_{\tilde{u}_k}) \right. \\ \left. + \delta_{ij} F_{kk'}^A \sqrt{x_{\chi_i^-}} f_{C^0}(x_{\chi_i^-}, x_{\tilde{u}_k}, x_{\tilde{u}_{k'}}) \right] , \quad (5.100)$$

$$C_{Q_1}^{BS} = -f_{ac} \frac{M_W}{m_b \tan \beta \lambda_t} \sum_{i,j=1}^2 \sum_{k=1}^6 \mathcal{H}_{jbbk} \Gamma_{isk}^\dagger \left(\sqrt{x_{\chi_i^-} x_{\chi_j^-}} Q_{ij} + x_{\tilde{u}_k} Q_{ij}^\dagger \right) f_{D^0}(x_{\chi_i^-}, x_{\chi_j^-}, x_{\tilde{u}_k}, x_{\tilde{\nu}_l}) \quad (5.101)$$

$$C_{Q_2}^{BS} = -f_{ac} \frac{M_W}{m_b \tan \beta \lambda_t} \sum_{i,j=1}^2 \sum_{k=1}^6 \mathcal{H}_{jbbk} \Gamma_{isk}^\dagger \left(\sqrt{x_{\chi_i^-} x_{\chi_j^-}} Q_{ij} - x_{\tilde{u}_k} Q_{ij}^\dagger \right) f_{D^0}(x_{\chi_i^-}, x_{\chi_j^-}, x_{\tilde{u}_k}, x_{\tilde{\nu}_l}) \quad (5.102)$$

where

$$f_{ac} = \frac{1}{4 \sin^2 \theta_w} \frac{m_b m_\ell}{M_W^2} \tan^2 \beta , r_{hH} = M_W^2 \left(\frac{\sin^2 \alpha}{M_{h^0}^2} + \frac{\cos^2 \alpha}{M_{H^0}^2} \right) , \quad (5.103)$$

$$r_A = \frac{M_W^2}{m_{A^0}^2} , x_{H^-} = \frac{m_{H^-}^2}{M_W^2} , x_t = \frac{m_t^2}{M_W^2} , x_{\chi_i^-} = \frac{m_{\chi_i^-}^2}{M_W^2} , x_{\tilde{u}_k} = \frac{m_{\tilde{u}_k}^2}{M_W^2} , \quad (5.104)$$

$$G_{ijk}^{hH} = \frac{M_W^2}{m_{h^0}^2} \sin \alpha (\sqrt{x_{\chi_i^-} x_{\chi_j^-}} g_{ijh^0}^+ + x_{\tilde{u}_k} g_{ijh^0}^-) - \frac{M_W^2}{m_{H^0}^2} \cos \alpha (\sqrt{x_{\chi_i^-} x_{\chi_j^-}} g_{ijH^0}^+ + x_{\tilde{u}_k} g_{ijH^0}^-) , \quad (5.105)$$

$$G_{ijk}^A = i \frac{M_W^2}{m_{A^0}^2} (\sqrt{x_{\chi_i^-} x_{\chi_j^-}} g_{ijA^0}^+ + x_{\tilde{u}_k} g_{ijA^0}^-) , \quad (5.106)$$

$$F_{kk'}^{hH} = \frac{M_W}{m_{h^0}^2} \sin \alpha f_{kk'h^0} - \frac{M_W}{m_{H^0}^2} \cos \alpha f_{kk'H^0} , F_{kk'}^A = i \frac{M_W}{m_{A^0}^2} f_{kk'A^0} . \quad (5.107)$$

The related loop-integral functions are defined as

$$F_3(x) = \frac{1}{2(x-1)^3} [x^2 - 4x + 3 + 2 \log x] , \quad (5.108)$$

$$F_4(x) = \frac{1}{2(x-1)^3} [x^2 - 1 - 2x \log x] , \quad (5.109)$$

$$F_9(x) = \frac{1}{2(x-1)^2} [x^2 - 7x + 6 + (3x+2) \log x] , \quad (5.110)$$

$$F_0(x, y) = \frac{1}{x-y} \left[\frac{x}{x-1} \log x - (x \rightarrow y) \right] , \quad (5.111)$$

$$G_0(x, y) = \frac{1}{x-y} \left[\frac{x^2}{x-1} \log x - \frac{3}{2}x - (x \rightarrow y) \right] , \quad (5.112)$$

$$G(x, y) = \frac{1}{x-y} \left[\frac{x^2}{x-1} \log x - \frac{1}{x-1} - (x \rightarrow y) \right] , \quad (5.113)$$

$$G'(x, y, z) = \frac{1}{x-y} [G_0(x, z) - G_0(y, z)] , \quad (5.114)$$

$$f_{B^0}(x, y) = \frac{1}{x-y} (x \log x - y \log y) , \quad (5.115)$$

$$f_{C^0}(x, y, z) = \frac{1}{y-z} (f_{B^0}(x, y) - f_{B^0}(x, z)) , \quad (5.116)$$

$$f_{D^0}(x, y, z, w) = \frac{1}{z-w} (f_{C^0}(x, y, z) - f_{C^0}(x, y, w)) . \quad (5.117)$$

In the above expressions for Wilson coefficients, the possible mixing among sneutrinos has been neglected.

References

- [1] F. Abe *et al.* (CDF collaboration), Phys. Rev. **D57**, 3811 (1998).
- [2] For a recent review and complete set of references see A.Ali, DESY 7-192, hep-ph/9709507
- [3] X. G. He, T. D. Nguyen and R. R. Volkas, Phys. Rev. **D38** (1988) 814.
- [4] W. Skiba and J. Kalinowski, Nucl. Phys. **B404** (1993) 3.
- [5] Y.-B. Dai, C.-S. Huang and H.-W. Huang, Phys. Lett. **B390** (1997) 257.
- [6] C.-S. Huang and Q.-S. Yan, Phys. Lett. **B442** (1998) 209.
- [7] C.-S. Huang, W. Liao and Q.-S. Yan, Phys. Rev. **D59** (1999) 011701.
- [8] S. R. Choudhury and N. Gaur, Phys. Lett. **B451** (1999) 86.
- [9] H.E. Logan and U. Nierste, hep-ph/0004139.

- [10] B.Grinstein, M.J.Savage and M.B.Wise, *Nucl.Phys.***B319** (1989)271.
- [11] Chao-Shang Huang, *Commun. Theor. Phys.* **2** (1983) 1265.
- [12] G. Buchalla, A.J. Buras and M.E. Lauthenbache, *Rev. Mod. Phys.* **68** (1996)1125.
- [13] T. Inami and C. S. Lim, *Prog. Theor. Phys.* **65**, 297 (1981) [erratum **65**, 1772 (1981)].
- [14] S. Bertolini, F. Borzumati, A. Masiero and G. Ridolfi, *Nucl. Phys.* **B353** (1991) 591.
- [15] F. Borzumati, hep-ph/9310212; N. Oshimo, *Nucl. Phys.* **B404** (1993) 20.
- [16] T.Goto,Y.Okada and Y. Shimizu *Phys. Rev.D* **58**(1998)094006
- [17] H. Georgi, *Hadronic Jour.* **1** (1978) 155.
- [18] J. F. Gunion, H. E. Haber, G. Kane and S. Dawson, *The Higgs Hunter's Guide* (Addison-Wesley, Reading, MA, 1990); errata hep-ph/9302272.
- [19] K.S. Babu and C. Kolda, *Phys. Rev. Lett.* **84** (2000) 228.
- [20] Y. Okada, M. Yamaguchi and T. Yanagida, *Prog. Theor. Phys.* **85** (1991)1; H. Haber and R. Hempfling. *Phys. Rev. Lett.* **66** 1815; J. Ellis, G. Ridolfi and F. Zwirner, *Phys. Lett.* **B257** (1991) 83.
- [21] M. Carena, M. Quiros and C. Wagner, *Nucl. Phys.* **B461** (1996) 407.
- [22] C.-S. Huang and S.-H. Zhu, *Phys. Rev.* **D60** (1999) 075012.
- [23] R. Garisto and J.N. Ng *Phys. Lett. B* 315 (1993) 372.
- [24] K. Pitts, *Proceedings 3th Workshop on Heavy Quarks at Fixed Target(HQ98)*, Batavia, USA.
- [25] S. Ahmed et.al, CLEO collaboration, CLEO CONF99-10, hep-ex/9908022.

Figure Captions

Fig. 1 Feynman diagrams which give the leading contributions to C_{Q_1} and C_{Q_2} in the 2HDM with large $\tan\beta$.

Fig. 2 Dominant Feynman diagrams in which the virtual superparticles are exchanged in the loop in MSSM with large $\tan\beta$.

Fig. 3 The branching ratio of $B_s \rightarrow \mu^+ \mu^-$ as functions of M_{H^0} in the 2HDM. Curves labelled by 1, 2, 3 corresponds to $\alpha = 0, \pi/8, \pi/4$ respectively. Other parameters are chosen to be $M_{h^0} = 120$ GeV, $M_{H^\pm} = 250$ GeV and $\tan\beta = 60$.

Fig. 4 The branching ratio as functions of α in the 2HDM. Four curves labelled by 1, 2, 3, 4 correspond to $M_{H^0} = 220, 320, 420, 520$ GeV respectively. Other parameters are the same in Fig. 3

Fig. 5 The branching ratio as functions of $\tan\beta$ with $\alpha = \pi/8$ in the 2HDM. Four curves are classified as in Fig. 4. Other parameters are chosen as in Fig. 3.

Fig. 6: The correlation between C_7 and C_{Q_1} for $l=\mu$ in MSSM with $m_{\tilde{t}_1}$, $m_{\tilde{t}_2}$, $m_{\tilde{e}_L}$, $m_{\chi_2^-}$ and $\tan\beta$ as free parameters.

Fig. 7: The correlation between C_7 and C_{Q_1} for $l=\tau$ in MSSM with $m_{\tilde{t}_1}$, $m_{\tilde{t}_2}$, $m_{\tilde{c}_L}$, $m_{\chi_2^-}$ and $\tan\beta$ as free parameters.

Fig. 8: $Br(B_s \rightarrow \mu^+\mu^-)$ as a function of C_{Q_1} in MSSM. $C_{Q_1} \approx -C_{Q_2}$ has been assumed. Three lines correspond to $C_9 = -4.2, -4.6, -5.0$ respectively.

Fig. 9: $Br(B_s \rightarrow \tau^+\tau^-)$ as a function of C_{Q_1} in MSSM. $C_{Q_1} \approx -C_{Q_2}$ has been assumed. Three lines correspond to $C_9 = -4.2, -4.6, -5.0$ respectively.

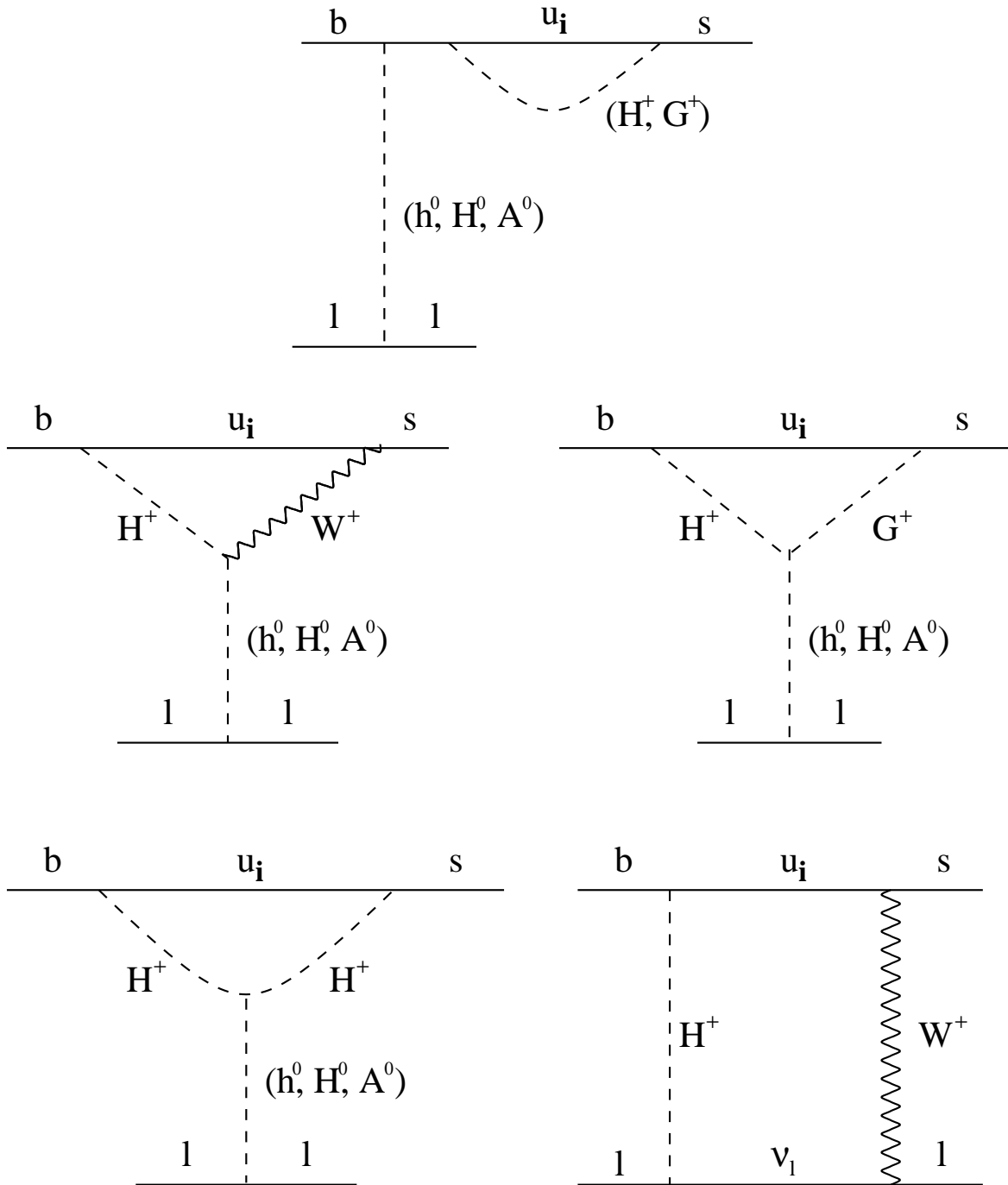


Figure 1:

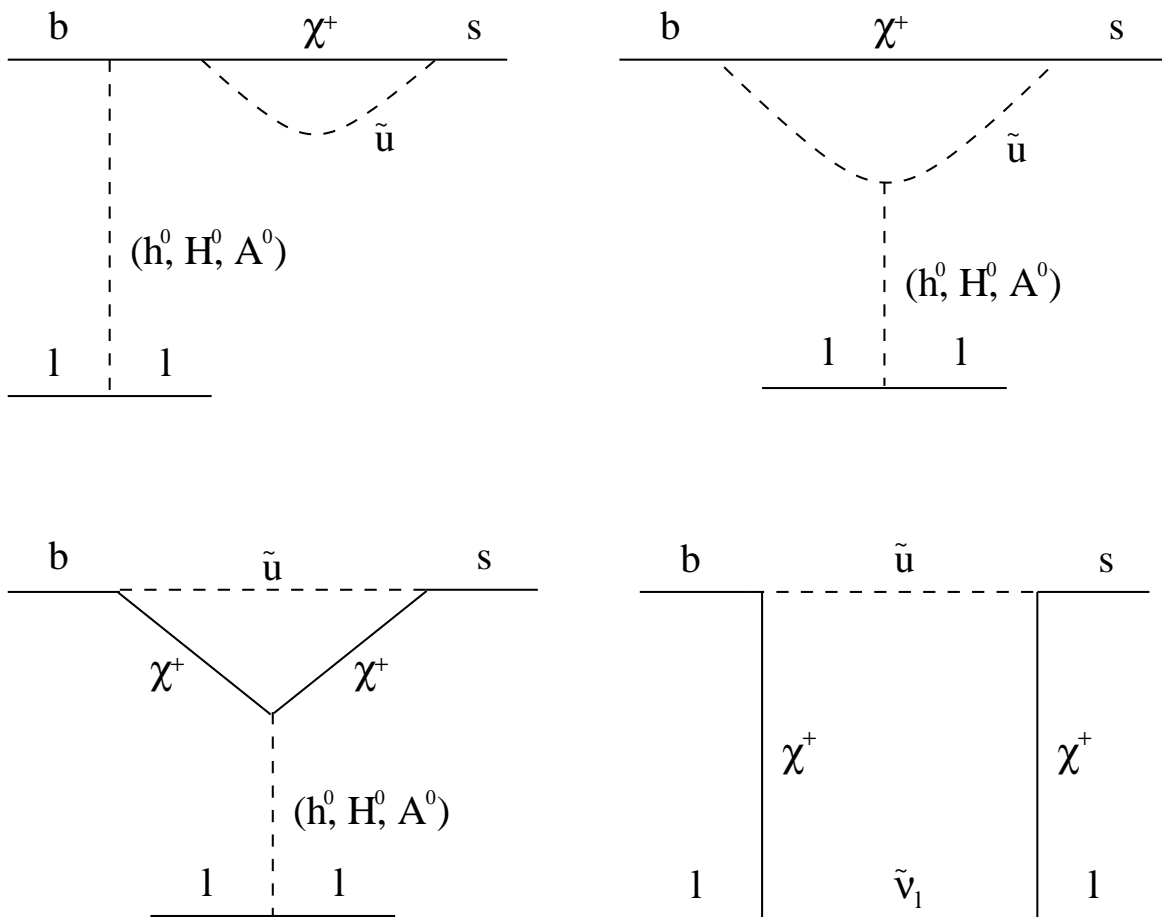


Figure 2:

Figure 3:

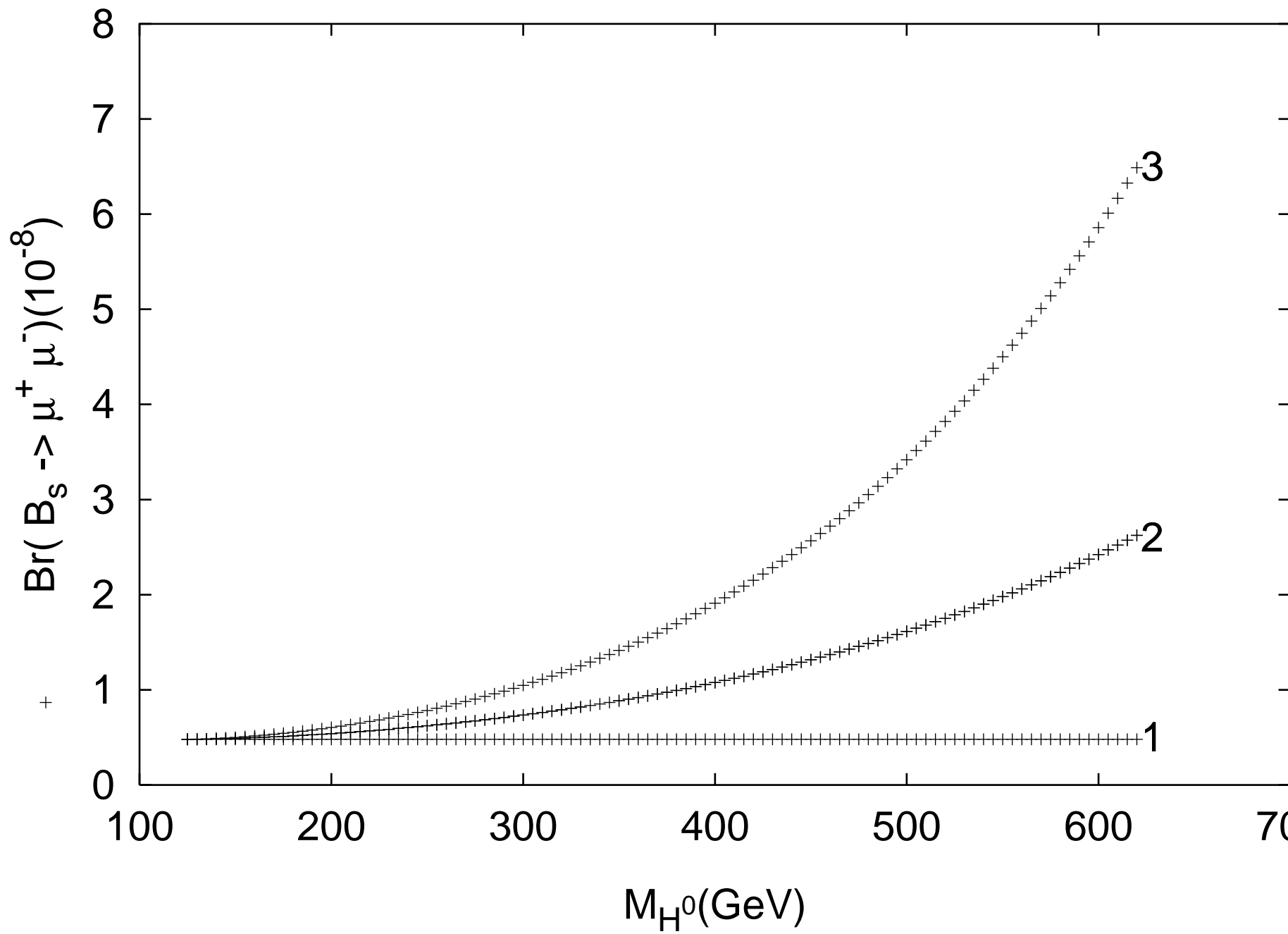


Figure 4:

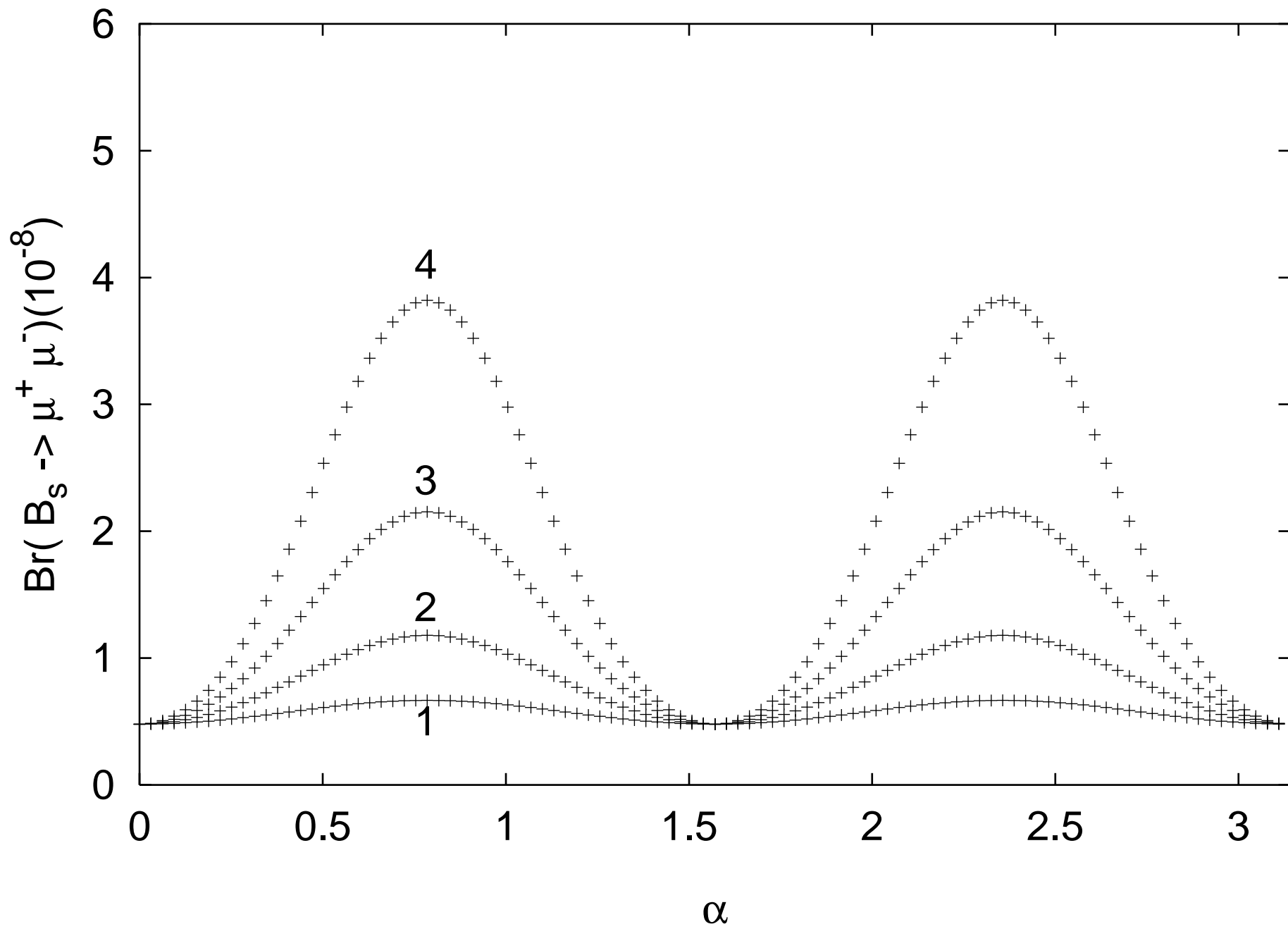
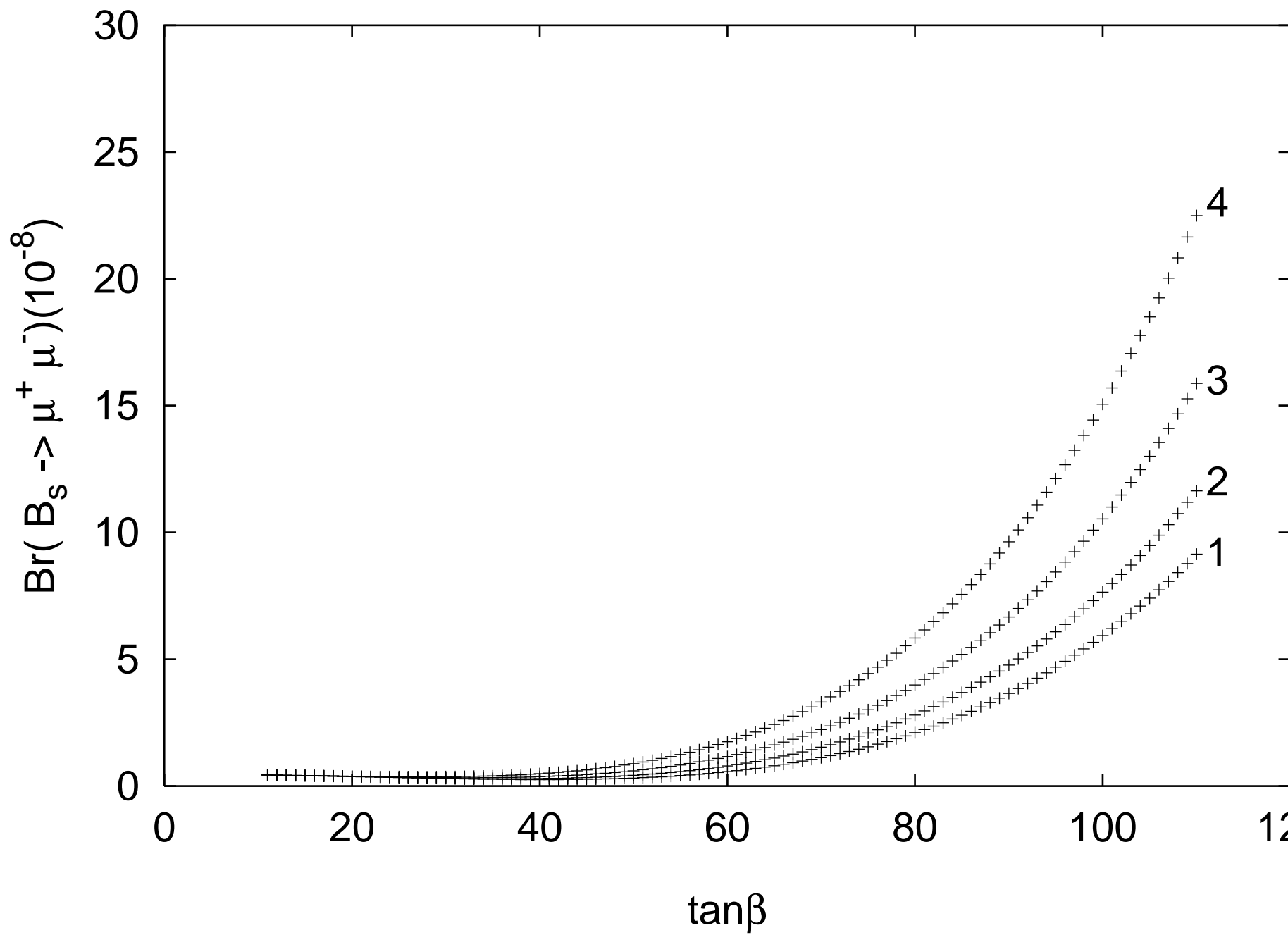


Figure 5:



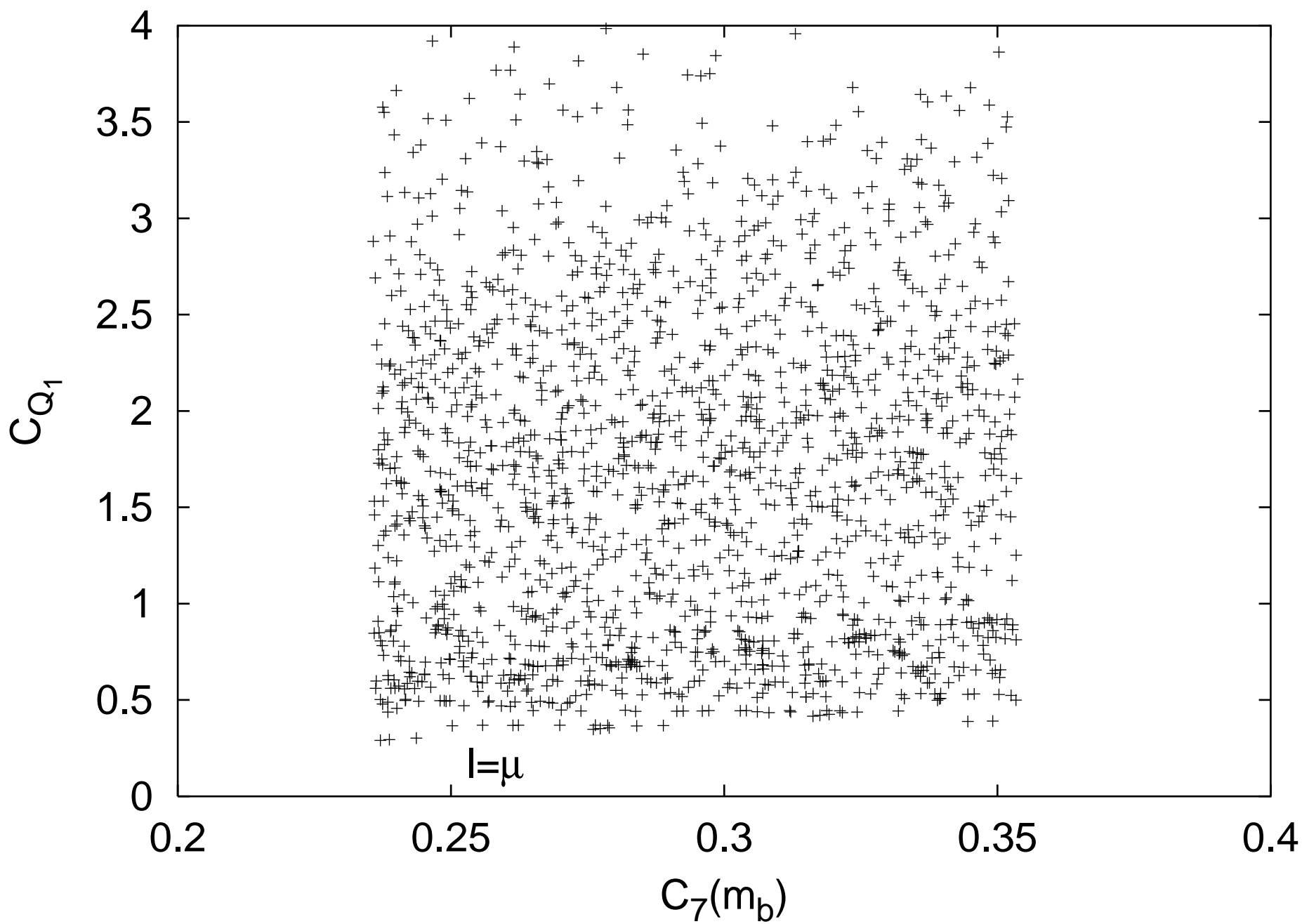


Figure 6:

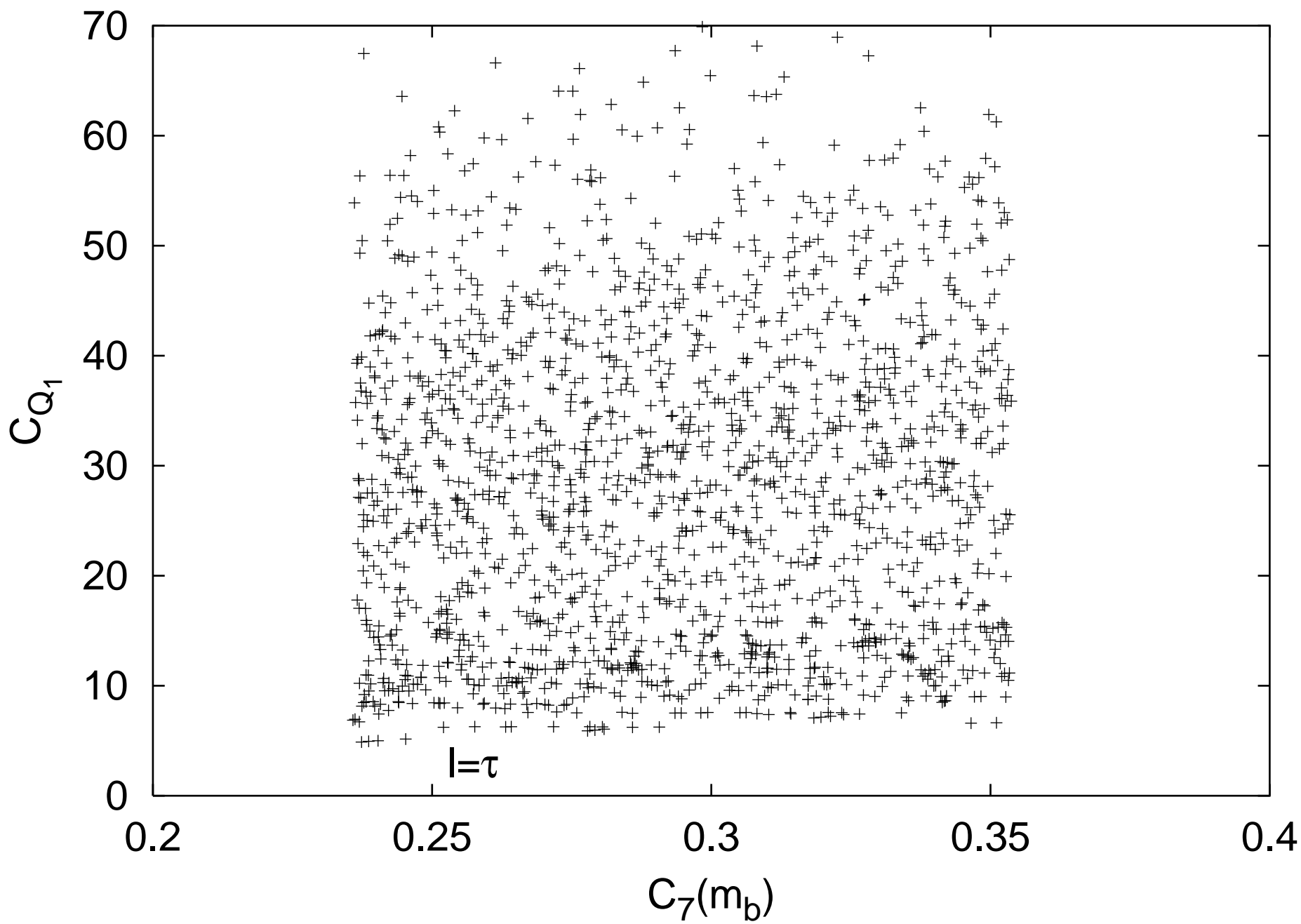


Figure 7:

Figure 8:

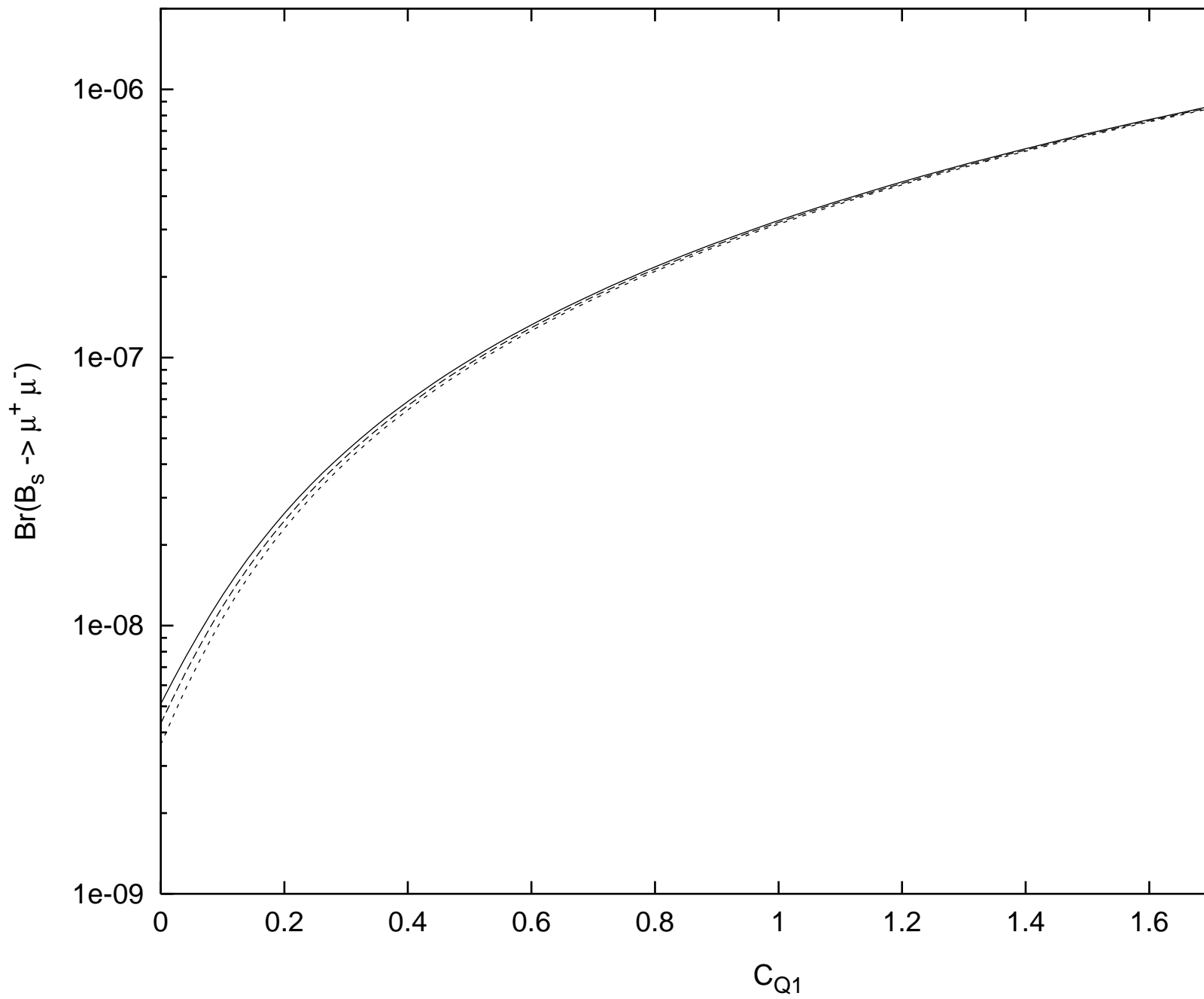


Figure 9:

